LANGMUIR Article
Cite This: Langmuir 2018, 34, 15174−15180
pubs.acs.org/Langmuir

Wettability of Amphoteric Surfaces: The Effect of pH and Ionic Strength on Surface Ionization and Wetting

Ettore Virga,[†,‡] Evan Spruijt,[§] Wiebe M. de Vos,*[,†] and P. M. Biesheuvel[‡]

[†]Membrane Science and Technology, University of Twente, Drienerlolaan 5, 7522 NB Enschede, The Netherlands
[‡]Wetsus, European Centre of Excellence for Sustainable Water Technology, Oostergoweg 9, 8911 MA Leeuwarden, The Netherlands
[§]Institute for Molecules and Materials, Radboud University, Heyendaalseweg 135, 6525 AJ Nijmegen, The Netherlands

ABSTRACT: We present a novel theory to predict the contact angle of water on amphoteric surfaces, as a function of pH and ionic strength. To validate our theory, experiments were performed on two commonly used amphoteric materials, alumina (Al_2O_3) and titania (TiO_2). We find good agreement at all pH values, and at different salt concentrations. With increasing salt concentration, the theory predicts the contact angle-pH curve to get steeper, while keeping the same contact angle at pH = PZC (point of zero charge), in agreement with data. Our model is based on the amphoteric 1-p*K* model and includes the electrostatic free energy of an aqueous system as well as the surface energy of a droplet in contact with the surface. In addition, we show how our theory suggests the possibility of a novel responsive membrane design, based on amphoteric groups. At pH ∼ PZC, this membrane resists flow of water but at slightly more acidic or basic conditions the wettability of the membrane pores may change sufficiently to allow passage of water and solutes. Moreover, these membranes could act as active sensors that only allow solutions of high ionic strength to flow through in wastewater treatment.

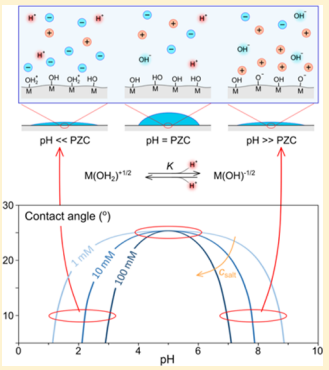

INTRODUCTION

Surface wettability is of key relevance in many applications in daily life[1−3] and industry.[4−6] The wettability of a surface results from a dynamic equilibrium between interaction forces taking place at solid−gas, solid−liquid, and gas−liquid interfaces.[1,7] By far the most common liquid involved in this balance is water. This balance can be shifted in many different ways.[8] For example, by changing pH, surfaces can be switched from hydrophilic to hydrophobic and back,[9] as demonstrated by various applications,[10,11] including new smart membranes with antifouling properties,[12] sponges for oil−water separation[13] and advanced drug delivery systems.[14] The possibility of switching results from weakly basic or acidic groups, of which the degree of ionization depends on solution pH.[15,16] Rios et al. exploit these material properties by developing membranes that are impermeable at neutral and basic conditions because of their hydrophobicity but are opened to a flux of aqueous solutions at slightly acidic pH because of protonation of amino groups, and subsequently wetting of the membrane pores.[17]

Within the class of ionizable materials, amphoteric surfaces are especially interesting. Amphoteric materials can be both positively and negatively charged, depending on pH in solution relative to their point of zero charge (PZC) (see Figure 1). The effects of pH and ionic strength on the wettability of amphoteric surfaces have already been experimentally investigated for titania (TiO_2) surfaces, coated with a thin silane layer (octadecyltryhydrosilane, OTHS), in a wide range of pH values around PZC.[18] For unmodified amphoteric surfaces, the effect of pH on wettability has only been investigated qualitatively for alumina (Al_2O_3) in order to determine PZC.[19] However, the role of the electrical double layer (EDL) on the wettability of amphoteric surfaces is not yet fully understood.[18] The salt concentration influences the diffuse part of the EDL, which in turn affects the surface charge and thereby the surface wettability. A quantitative understanding of the impact of the characteristics of the EDL on the surface energy of amphoteric solids is still missing.

In addition to theoretical challenges, earlier experimental work may not have chosen the best possible method to measure contact angle. Indeed, when contact angle (CA) measurements are based on the sessile drop technique,[20] the effect of a change in droplet pH during measurements may have been underestimated. Because when a droplet of water is placed on a solid surface, the ionization of the surface groups in such a small liquid volume can easily lead to a change of droplet pH. We advocate to work with the captive bubble technique, in which small volume effects can safely be neglected, as water constitutes the continuous phase with a large volume.

In this paper, we present a novel theory to predict the contact angle of water on amphoteric surfaces, as a function of pH and ionic strength. To validate our theory, we performed experiments on two commonly used amphoteric materials, alumina (Al_2O_3) and titania (TiO_2).

Received: August 30, 2018
Revised: October 11, 2018
Published: November 14, 2018

DOI: 10.1021/acs.langmuir.8b02875
Langmuir 2018, 34, 15174−15180

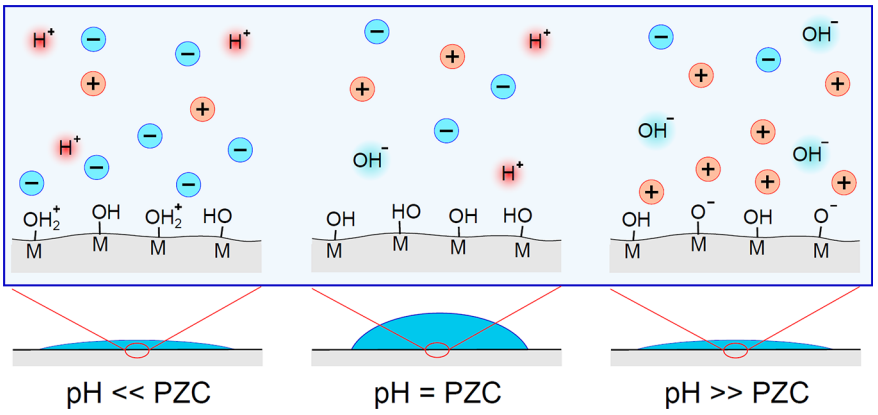

Figure 1. Illustration of the wettability of amphoteric materials in response to pH relative to the PZC.

THEORY

In this section, starting from general expressions for isolated ionizable surfaces,[21] we derive an equation that relates the water contact angle to the sum of surface and diffuse electrostatic free energies. Free energies discussed in this work have an electrical origin, due to the formation of the EDL, as well as a chemical origin, due to the adsorption/desorption of protons and ions to/from the surface. A possible Stern layer[22] is neglected in this work. Our system consists of a liquid interacting with a solid ionizable surface that is not soluble in that liquid. Because the Gibbs energy and Helmholtz energy are identical for a system in which the redistribution of ions (which is required for the formation of EDLs) does not affect the volume, the general term free energy is used here. The equations below are derived for an electrolyte with monovalent ions only. The electrostatic free energy, scaled with kT, of an aqueous system containing a ionizable surface is given by[21]

$$F_{el} = F_S + F_D \tag{1}$$

where F_S and F_D are the surface and the diffuse contributions to the electrostatic free energy.

The diffuse contribution for an isolated surface is given by[23]

$$F_D = -16 n_\infty \lambda_D \sinh^2\left(\frac{1}{4} y_s\right) \tag{2}$$

where n_∞ is the salt concentration expressed in m^{-3} ($n_\infty = N_{av} c_\infty$, with c_∞ in mol/m^3 = mM and N_{av} Avogadro's number), and the Debye length λ_D is given by

$$\lambda_D = \sqrt{\frac{\varepsilon kT}{2e^2 n_\infty}} \tag{3}$$

with e as the elementary charge, ε is the dielectric constant ($= \varepsilon_r \varepsilon_0 = 78{\cdot}8.854 \times 10^{-12}$ C/(V m) in water), k is the Boltzmann constant, and T is temperature.

In order to calculate F_{el}, we also need to know the surface contribution, F_S. The expression for F_S depends on the surface chemistry.[21] For an acidic or basic material, the ionization degree α is a number in between 0 and 1 and is given by[21]

$$\alpha = \frac{1}{1 + e^{z(y_N - y_s)}} \tag{4}$$

where z is the charge sign of the surface groups (for an acidic site, $z = -1$, and for a basic site, $z = +1$), y_s is the dimensionless electrostatic potential at the surface ($= e\psi_s/kT$, with ψ_s as the electrostatic potential at the surface), and where y_N is given by[21]

$$y_N = \ln 10 \cdot (pK - pH) \tag{5}$$

For an acidic/basic material for which ionization is described by eq 4, the surface part of the free energy, F_S, is given by[21]

$$F_S = N \cdot \ln(1 - \alpha) \tag{6}$$

where N is the number density of ionizable groups on the surface (m^{-2}). One class of amphoteric materials consists of a mixture of acidic and basic surface groups. In that case, the above theory applies with eqs 4–6 evaluated for each group separately (and added up). This approach can be applied to various biological materials, such as protein molecules, the surface of which consists of an assembly of basic and acidic groups.[24]

In the present work, we focus on a second class of amphoteric materials, that includes as examples titania and alumina. For these materials, it is known that they have a fractional charge which goes from a number below zero, to above. For alumina, applying the 1-pK model, the surface consists of $OH^{-1/2}$ groups that can be protonated to $OH_2^{+1/2}$ groups.[25,26] In this case the pK of this material is the pH at which the surface is globally uncharged. The effective surface charge, α ($-\frac{1}{2} < \alpha < +\frac{1}{2}$), is obtained from

$$\alpha = \frac{1}{2} - \frac{1}{1 + e^{y_N - y_s}} \tag{7}$$

and, as shown in ref 10, the surface contribution to the free energy in this case is

$$F_S = \frac{1}{2} N \ln((1 + 2\alpha)(1 - 2\alpha)) \tag{8}$$

Combining eq 2 and eq 8, we can now rewrite eq 1 for this amphoteric material to

$$F_{el} = \frac{1}{2} N \ln((1 + 2\alpha)(1 - 2\alpha)) - 16 n_\infty \lambda_D \sinh^2\left(\frac{1}{4} y_s\right) \tag{9}$$

According to Hiemstra et al.,[26] titania is different from alumina, because titania has two ionizable groups, one that goes from −2/3 to +1/3 in charge, the other from −1/3 to +2/3. However, because the pK value of both groups can be assumed to be the same, and the number of groups can also be assumed to be the same,[26] after adding up these groups we obtain the same equations for α and F_S as for alumina (i.e., eqs

DOI: 10.1021/acs.langmuir.8b02875
Langmuir 2018, 34, 15174−15180

7 and 8). Equation 8 was derived in ref 10 but not tested experimentally before, and this test is one of the objectives of the present work.

In order to calculate F_{el}, the value of surface potential y_s is needed. To that end, we solve the 1D Poisson–Boltzmann equation for a planar surface,

$$\frac{\partial^2 y}{\partial x^2} = \frac{\sinh y}{\lambda_D^2} \tag{10}$$

with the boundary condition

$$\left.\frac{\partial y}{\partial x}\right|_s = -\frac{e^2\sigma}{\varepsilon kT} \tag{11}$$

where the number density of charged groups σ in m^{-2} is given by $\sigma = \alpha N$. For isolated surfaces the solution of eq 10 is well-known to be[27]

$$\sigma = n_\infty \lambda_D \sqrt{8(\cosh y_s - 1)} \tag{12}$$

By solving eq 12 with an expression for α, such as eq 7, both y_s and α are obtained.

F_{el} can be seen as an electrostatic contribution to the free energy per unit of surface area, or the solid–liquid surface energy, which has units mN/m when multiplied by kT. From this point onward, we refer to it as the electrostatic contribution to the surface energy, γ_{el}.

For smooth surfaces, the different surface energies are related to the static contact angle by Young's equation,

$$\gamma_{lg}\cdot\cos\theta = \gamma_{sg} - \gamma_{sl} \tag{13}$$

where γ_{sl}, γ_{sg}, and γ_{lg} refer to the surface energy of the solid–liquid, solid–gas, and liquid–gas interface, respectively. In particular, we can think of γ_{sl} as sum of an electrostatic term, γ_{el}, and a nonelectrostatic term, γ_{sl}^{pzc} (value of γ_{sl} when the material is uncharged, i.e., when pH = PZC)

$$\gamma_{sl} = \gamma_{sl}^{pzc} + \gamma_{el} \tag{14}$$

Thus, eq 113 can be rewritten to

$$\gamma_{lg}\cdot\cos\theta = \Delta\gamma - \gamma_{el} \tag{15}$$

where $\Delta\gamma = \gamma_{sg} - \gamma_{sl}^{pzc}$. The value of γ_{lg}, the surface energy of the water–air (liquid–gas) interface has been fixed in our study to a value of to γ_{lg} = 73 mN/m.[28] The term $\Delta\gamma$ is independent of pH and salt concentration and can be obtained by experimental data fitting. This means that if the contact angle at the point of zero charge is known, the model allows us to predict values of contact angle for every other value of pH and ionic strength. This is correct only if these parameters (pH and ionic strength) have a reversible effect on the surface chemistry hence on the dissociation of surface groups.

MATERIALS AND METHODS

Chemicals. For preparation of the solutions at different ionic strength, we used Milli-Q water and NaCl. We added small quantities of 1 M NaOH or HCl (37%) in order to obtain the desired solution pH. We tested two materials, alumina and titania, supplied respectively as sapphire and rutile. Sapphire (1ALO 402E, Al_2O_3 substrate (0001)) and rutile (1TIO 109E, TiO_2 substrate (100)) were supplied by Crystal GmbH (Berlin, Germany). These substrates are polished (on one side, $R < a0.5$ nm) and have dimensions 10 × 10 × 0.5 mm^3. To improve the measurement of the contact angle, a customized sample holder was designed and constructed (PLA, 3D printing, Ultimaker^{2+}, Geldermalsen, The Netherlands) (see Figure 2), as discussed next.

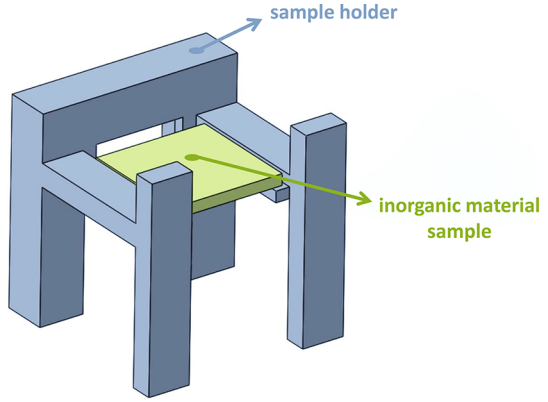

Figure 2. Illustration of 3D printed sample holder (blue) containing a sample of inorganic material (10 × 10 × 0.5 mm^3) (green).

Contact Angle Measurements. In order to obtain a higher control on the water solution properties, the static contact angle was measured using the captive bubble approach. The advantage of this technique compared to the more common sessile drop method is that the volume of the surrounding aqueous solution is much larger than that of a single droplet, and thus pH and salt concentration will be much more stable. Another important advantage of the captive bubble method, relatively to the method where a droplet is placed on top of the material (sessile drop), is that in the captive bubble approach, the gas phase humidity is well-controlled.

The sample surface was first flushed with ethanol (70%) and then with Milli-Q water before every measurement. Then, the sample was placed into the 3D printed sample holder with its polished side facing downward and submerged in an aqueous solution of predetermined ionic strength and pH. Before measuring the contact angle, the sample was left in contact with the solution for at least 5 min and only then we injected a gas bubble from below, displacing water from part of the surface.

The measurements were performed with an instrument for contact angle and contour analysis (OCA 35, Dataphysics, Filderstadt, Germany) used to measure the static contact angle. A clean stainless steel needle was used to produce a bubble of ~3 mm in diameter on the surface, and the bubble contour, measured through the aqueous phase, was recorded. At least five measurements were taken for every condition. Image analysis of the shapes of the air bubbles were performed with the software provided with the instrument by using the method of Young–Laplace fitting.

RESULTS AND DISCUSSION

In this section, we compare our model predictions to experimental data from literature, and compare to data obtained in our own experiments. Subsequently, we will discuss more detailed predictions on how amphoteric surfaces can inspire the design of a responsive membrane that acts as a sensor for the quality of the water in wastewater treatment plants, allowing, streams at high ionic strength to flow through and go directly to appropriate disposal units. In this design the membrane would thus act as both a sensor and a valve, with the ability to react to a change in water chemistry automatically and in an autonomic fashion.

Our model prediction are compared with experimental data found in literature[18] for a silanized titania surface (54% OTHS) and are shown in Figure 3.

According to our model fit, the contact angle (CA) has a maximum for pH = 4.4 (PZC of titania[18]), while CA decreases

DOI: 10.1021/acs.langmuir.8b02875
Langmuir 2018, 34, 15174–15180

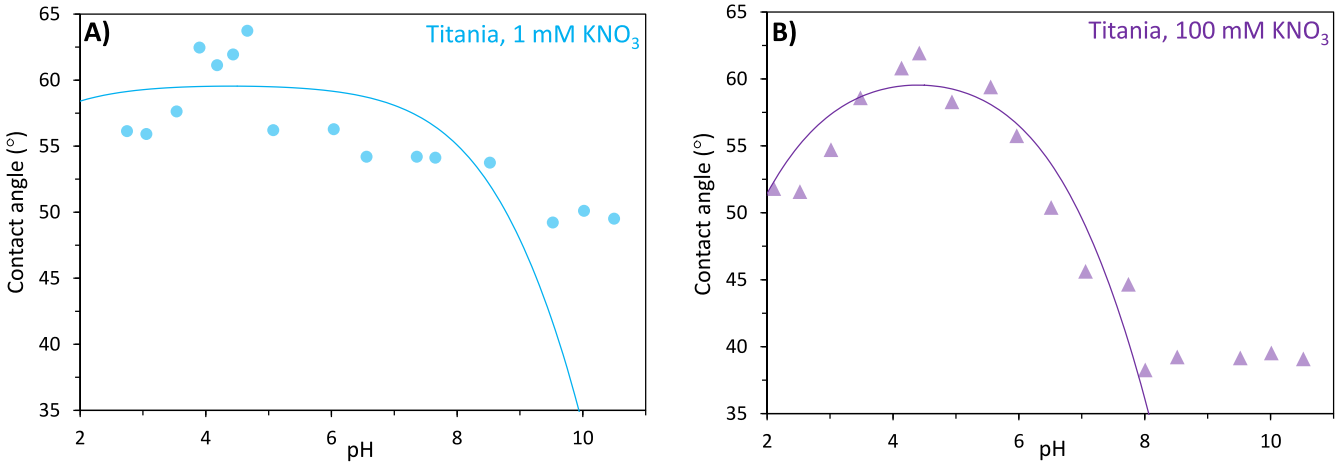

Figure 3. Contact angle of water on a partially silanized titania wafer in c_∞ = 1 mM (A) and 100 mM (B) KNO_3 as a function of pH. Experiments[18] (symbols) and theory (lines) based on eqs 5, 7, 9, 12, and.15 Input model parameters: N = 3.0 nm^{-2},[18] pK = 4.4,[18] $\Delta\gamma$ = 37 mN/m.

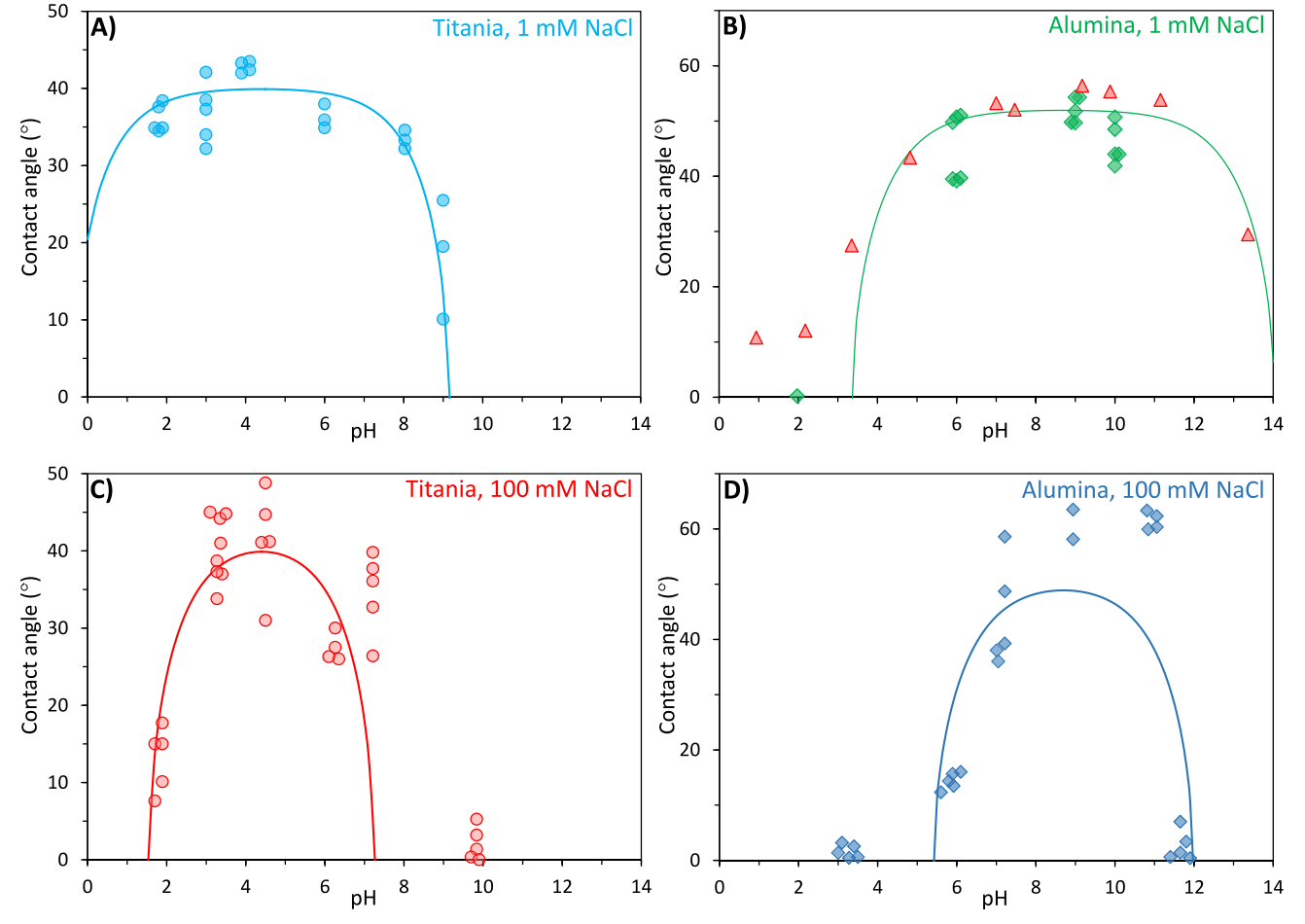

Figure 4. Contact angle of water on titania in c_∞ = 1 mM (A) and 100 mM (B), and alumina, in c_∞ = 1 mM (C) and 100 mM (D), substrates as a function of pH. Experiments (circles and diamonds [this work], and triangles [Cuddy et al.]) and theory (lines). Input model parameters for titania: N = 8.0 nm^{-2},[18] pK = 4.4,[18] $\Delta\gamma$ = 56 mN/m. Input model parameters for alumina: N = 7.25 nm^{-2},[29] pK = 8.7,[19] $\Delta\gamma$ = 45 mN/m.

when pH moves away from PZC. Indeed, when we move pH away from PZC, the surface becomes more charged due to the ionization of surface groups, thus it becomes more hydrophilic. We also observe that when the salt concentration is increased, from 1 mM (Figure 3A) to 100 mM (Figure 3B), the steepness of the curve of contact angle versus pH increases considerably. This can be explained by the influence of salt concentration on the Debye length λ_D, thus on the EDL thickness. An increase in ionic strength leads to a reduction in EDL thickness, which translates into a concentration of H^+ or OH^- at the surface that is much closer to the one in the bulk. Thus, for an amphoteric material, if we increase the ionic strength, keeping the pH constant, the ionization of the surface groups will increase.

DOI: 10.1021/acs.langmuir.8b02875
Langmuir 2018, 34, 15174−15180

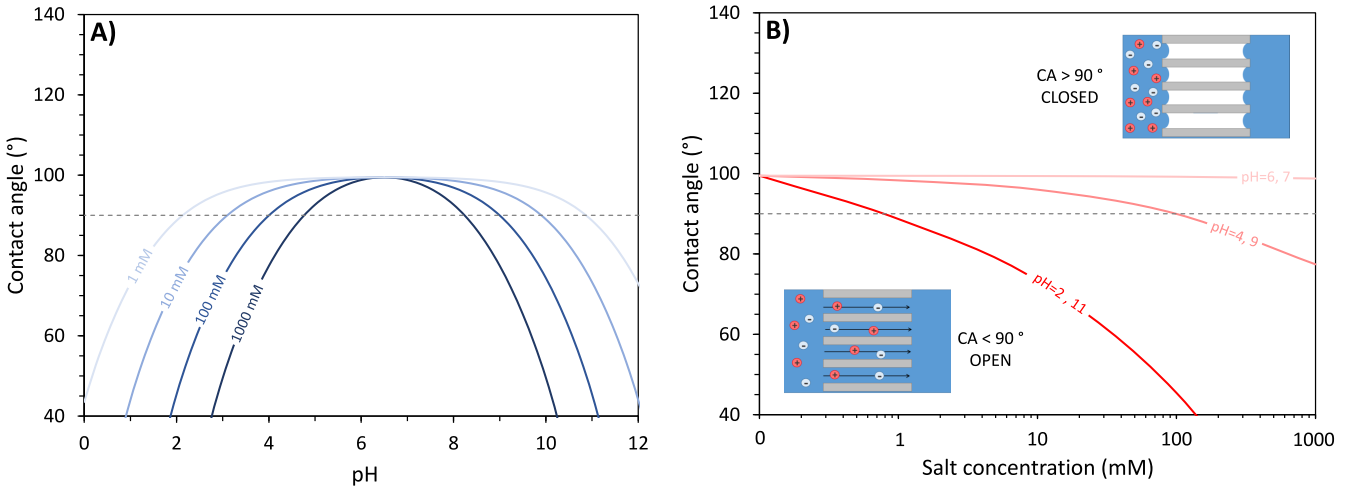

Figure 5. Predictions of water contact angle on an intrinsically hydrophobic membrane with amphoteric groups as a function of pH and ionic strength. Input model parameters: N = 8.0 nm^{-2}, pK = 6.5, $\Delta\gamma$ = −12 mN/m.

It is possible to note a plateau at high pH in the experimental results collected by Hanly et al. (CA∼ 50° in Figure 3A and CA∼ 40° in Figure 3B). This behavior differs from our predictions at high pH. It can possibly be explained by looking at the composition of the surfaces studied by Hanly et al., namely titania partially covered with OTHS (54%). The hydrophobic interactions due to the silane coverage of titania are not taken into account in our model and these may be responsible for the observed plateau at high pH.

To validate our model against data for amphoteric surfaces without hydrophobic modifications, we collected experimental data for the CA of two surfaces, titania and alumina, at different values of pH and ionic strength. Model predictions and experimental data are shown in Figure 4 for a concentration of NaCl equal to c_∞ = 1 mM. As can be observed in Figure 4A, also in this case the contact angle has a maximum for titania at pH ≅ 4.4, while for alumina, Figure 4B, the maximum is at pH ≅ 8.7 (PZC of alumina[19]), and in both cases the contact angle decreases when the pH moves away from PZC.

In Figure 4B, we also show data collected by Cuddy et al.[19] (triangles) for alumina. Cuddy et al. used the sessile drop technique and worked initially with deionized water. Thus, as discussed previously the exact salt concentration of their aqueous phase (after contacting the surface) is unknown. Their data overlap with our data (see Figure 4B) and therefore, our model calculations, based on c_∞ = 1 mM, fit their data well.

In our model, for an amphoteric material the contact angle has a maximum for a value of pH equal to pK, which is the point where the surface is on average uncharged (for these materials), that is, the PZC. When we move pH away from PZC, the surface becomes more charged due to the ionization of surface groups, thus it becomes more hydrophilic and CA decreases. Next, in Figure 5A, we show how water contact angle changes if both pH and ionic strength are varied. When salt concentration is increased, the contact angle at the PZC is expected to be unchanged, in line with literature data reported for titania (see Figure 3). Shifting pH away from PZC, our model predicts that the influence of ionic strength on contact angle becomes increasingly prominent. One may, indeed, observe an increased curves steepness when ionic strength is increased. Indeed, an increase in ionic strength leads to a reduction in EDL thickness, that translates into a concentration of H^+ or OH^- at the surface closer to the one in the bulk. Thus, if we increase ionic strength, keeping pH constant, the ionization of the surface groups will increase.

These trends of the dependence of CA on salt concentration are confirmed by Hanly et al.[18] and by our own experiments at 100 mM salinity (see Figure 4C,D). The experimental data show an increase in steepness of the curve for CA, if compared to low salt concentration, such as 1 mM (see Figure 4). This is in line with the theory where we can observe a decrease of the pH region delimited by our theoretical lines.

As already mentioned above, our theory shows that if we keep pH constant and away from PZC, an increase in ionic strength leads to an increase in surface hydrophilicity (see Figure 5A). On the basis of that prediction, we can now think of the possibility of a membrane, where the ionic strength determines the permeability. These membranes will be analogous to the ones already developed by Rios et al.[17] but also more versatile. Their modified membranes are dry at neutral and basic conditions because of their hydrophobicity but open to flux of aqueous solutions at slightly acidic pH because of the protonation of amino groups. The same response is expected by switching the ionic strength at constant pH (away from the PZC). Thus, the corresponding membranes will perform as ionic strength-dependent switchable valves. If an intrinsically hydrophobic membrane with amphoteric groups is employed, it will resist flow of water through the pores of the membrane at pH ∼ PZC, but at slightly more acidic or basic conditions, the wettability of the membrane pores may change sufficiently to allow passage of water and ions. As explained in ref 30, the boundary between an open and closed configuration is at value of CA = 90° for ideal surfaces. Indeed, by varying the contact angle (when CA > 90°) we are able to show in theory that the critical pressure needed to push the water through a membrane can be varied. But, when CA < 90° we ideally do not need any difference in pressure between the two sides of the membrane in order to make water pass through it.[30] Thus, operating below the critical pressure, it is possible to open and close ideal membrane pores by shifting the surface from hydrophobic to hydrophilic. These membranes will be able to work in a much larger range of pH (Figure 5A), then the membranes described by Rios et al. Our model predicts that these membranes could possibly act as active sensors that only allow solutions of high

DOI: 10.1021/acs.langmuir.8b02875
Langmuir 2018, 34, 15174−15180

ionic strength to flow through. This would be especially useful for wastewater treatment, when the ionic strength and/or pH of the water vary strongly in time. Streams with a more extreme pH or a high salt concentration would permeate through the membrane and be treated, while low salinity streams with moderate pH could simply be disposed. If we look at Figure 5B, we can see the effect of salt concentration when pH is kept constant. For pH values too close to the PZC, such as pH = 6 and pH = 7, this shift from hydrophobic to hydrophilic is not possible. But when pH is sufficiently far away from PZC, by changing the ionic strength it becomes possible to switch the membrane surface from hydrophobic to hydrophilic. This effect increases when pH is increasingly different from the PZC of the membrane, that we fixed to PZC = pK = 6.5 in this calculation. The high contrast between the open and closed states, as well as high fluxes in the open state because of a large pore size[17] can be useful in different applications for ionic strength/pH switchable membranes.

CONCLUSIONS

This study focused on the effects of pH and ionic strength on the wettability of amphoteric metal oxide surfaces. We studied the contact angle of water on two oxidic (inorganic) materials: alumina (Al_2O_3) and titania (TiO_2). We present a novel theory that is able to predict the contact angle for these materials as a function of both ionic strength and pH. This theory is based on the amphoteric 1-pK model. Experimentally, we work with the captive bubble technique which gives a better control over solution and air properties. Data were very well described by the new theory for the lowest salt concentration tested (1 mM NaCl) and their trend confirmed also at high salt concentration (100 mM). For higher salt concentration, the theory predicts the contact angle-pH curve to get steeper, while keeping the same contact angle at pH = PZC. Both literature data and our own experiments do show this effect, thus in line with our theory. Indeed, our theory shows that, if we keep pH constant, away from PZC, an increase in ionic strength leads to an increase in hydrophilicity. Thus, if an intrinsically hydrophobic membrane with amphoteric groups is employed, it will resist the flow of water through the membrane at pH ∼ PZC but at slightly more acidic or basic conditions the wettability of the membrane pores may change sufficiently to allow passage water and ions. These membranes could also act as valves that only allow solutions of high ionic strength to flow through. The high contrast between the open and closed states can be particularly useful for water treatment.

AUTHOR INFORMATION

Corresponding Author

*E-mail: w.m.devos@utwente.nl.

ORCID

Ettore Virga: 0000-0002-9304-3784

Wiebe M. de Vos: 0000-0002-0133-1931

P. M. Biesheuvel: 0000-0002-5468-559X

Notes

The authors declare no competing financial interest.

ACKNOWLEDGMENTS

This work was performed in the cooperation framework of Wetsus, European Centre of Excellence for Sustainable Water Technology (www.wetsus.nl). Wetsus is cofunded by the Dutch Ministry of Economic Affairs and Ministry of Infrastructure and Environment, the European Union Regional Development Fund, the Province of Fryslân and the Northern Netherlands Provinces. This work is part of a project that has received funding from the European Union's Horizon 2020 research and innovation programme under the Marie Skłodowska-Curie Grant Agreement 665874. The authors thank the participants of the research theme "Concentrates" for fruitful discussions and financial support. The authors also thank Jan Jurjen Salverda for his contribution in the realization of the 3D-printed sample holder.

REFERENCES

(1) Kondyurin, A.; Bilek, M. *Ion Beam Treatment of Polymers*, second ed.; Elsevier, 2015; pp 129 − 143.

(2) Feng, L.; Li, S.; Li, Y.; Li, H.; Zhang, L.; Zhai, J.; Song, Y.; Liu, B.; Jiang, L.; Zhu, D. Super-Hydrophobic Surfaces: From Natural to Artificial. *Adv. Mater.* **2002**, *14*, 1857−1860.

(3) Barthlott, W.; Mail, M.; Neinhuis, C. Superhydrophobic hierarchically structured surfaces in biology: evolution, structural principles and biomimetic applications. *Philos. Trans. R. Soc., A* **2016**, *374*, 20160191.

(4) Salathiel, R. A. Oil Recovery by Surface Film Drainage In Mixed-Wettability Rocks. *JPT, J. Pet. Technol.* **1973**, *25*, 1216−1224.

(5) Tanaka, T.; Lee, J.; Scheller, P. R. *Treatise on Process Metallurgy*; Elsevier, 2014; pp 61 − 77.

(6) Zhou, Y.-N.; Li, J.-J.; Luo, Z.-H. Toward efficient water/oil separation material: Effect of copolymer composition on pH-responsive wettability and separation performance. *AIChE J.* **2016**, *62*, 1758−1771.

(7) Park, S.-J.; Seo, M.-K. *Interface Science and Composites*; Interface Science and Technology; Elsevier, 2011; Vol. *18*; pp 147−252.

(8) Verplanck, N.; Coffinier, Y.; Thomy, V.; Boukherroub, R. Wettability Switching Techniques on Superhydrophobic Surfaces. *Nanoscale Res. Lett.* **2007**, *2*, 577−596.

(9) Xia, F.; Zhu, Y.; Feng, L.; Jiang, L. Smart responsive surfaces switching reversibly between super-hydrophobicity and super-hydrophilicity. *Soft Matter* **2009**, *5*, 275−281.

(10) Nunes, S. P.; Behzad, A. R.; Hooghan, B.; Sougrat, R.; Karunakaran, M.; Pradeep, N.; Vainio, U.; Peinemann, K.-V. Switchable pH-Responsive Polymeric Membranes Prepared via Block Copolymer Micelle Assembly. *ACS Nano* **2011**, *5*, 3516−3522.

(11) Chen, X.; Gao, J.; Song, B.; Mario, S.; Zhang, X. Stimuli-Responsive Wettability of Nonplanar Substrates: pH-Controlled Floatation and Supporting Force. *Langmuir* **2010**, *26*, 104−108.

(12) Cai, Y.; Chen, D.; Li, N.; Xu, Q.; Li, H.; He, J.; Lu, J. A smart membrane with antifouling capability and switchable oil wettability for high-efficiency oil/water emulsions separation. *J. Membr. Sci.* **2018**, *555*, 69−77.

(13) Guo, J.; Wang, J.; Gao, Y.; Wang, J.; Chang, W.; Liao, S.; Qian, Z.; Liu, Y. pH-Responsive Sponges Fabricated by Ag−S Ligands Possess Smart Double-Transformed Superhydrophilic−Superhydrophobic−Superhydrophilic Wettability for Oil−Water Separation. *ACS Sustainable Chem. Eng.* **2017**, *5*, 10772−10782.

(14) Salinas, Y.; Castilla, A. M.; Resmini, M. An l-proline based thermoresponsive and pH-switchable nanogel as a drug delivery vehicle. *Polym. Chem.* **2018**, *9*, 2271−2280.

(15) Aguilar, M. R.; Román, J. S. *3 - pH-responsive polymers: properties, synthesis and applications*; Woodhead Publishing, 2014; Vol. *1*, pp 45−92.

(16) Kocak, G.; Tuncer, C.; Butun, V. pH-Responsive polymers. *Polym. Chem.* **2017**, *8*, 144−176.

(17) Rios, F.; Smirnov, S. N. pH Valve Based on Hydrophobicity Switching. *Chem. Mater.* **2011**, *23*, 3601−3605.

(18) Hanly, G.; Fornasiero, D.; Ralston, J.; Sedev, R. Electrostatics and Metal Oxide Wettability. *J. Phys. Chem. C* **2011**, *115*, 14914−14921.

(19) Cuddy, M. F.; Poda, A. R.; Brantley, L. N. Determination of Isoelectric Points and the Role of pH for Common Quartz Crystal

DOI: 10.1021/acs.langmuir.8b02875
Langmuir 2018, 34, 15174−15180

Microbalance Sensors. *ACS Appl. Mater. Interfaces* **2013**, *5*, 3514−3518.
(20) Shahidzadeh, N.; Schut, M. F. L.; Desarnaud, J.; Prat, M.; Bonn, D. Salt stains from evaporating droplets. *Sci. Rep.* **2015**, *5*, 10335.
(21) Biesheuvel, P. M. Electrostatic free energy of interacting ionizable double layers. *J. Colloid Interface Sci.* **2004**, *275*, 514−522.
(22) Travesset, A.; Vangaveti, S. Electrostatic correlations at the stern layer: physics or chemistry? *J. Chem. Phys.* **2009**, *131*, 185102.
(23) Chan, D. Y. C.; Mitchell, D. The free energy of an electrical double layer. *J. Colloid Interface Sci.* **1983**, *95*, 193−197.
(24) de Vos, W. M.; Biesheuvel, P. M.; de Keizer, A.; Kleijn, J. M.; Cohen Stuart, M. A. Adsorption of the Protein Bovine Serum Albumin in a Planar Poly(acrylic acid) Brush Layer As Measured by Optical Reflectometry. *Langmuir* **2008**, *24*, 6575−6584.
(25) Koopal, T. A. J. Ionized monolayers. *Philips Res. Rep.* **1955**, *10*, 425−481.
(26) Hiemstra, T.; De Wit, J.; Van Riemsdijk, W. Multisite proton adsorption modeling at the solid/solution interface of (hydr)oxides: A new approach: II. Application to various important (hydr)oxides. *J. Colloid Interface Sci.* **1989**, *133*, 105−117.
(27) Virga, E.; De Vos, W. M.; Biesheuvel, P. M. Theory of gel expansion to generate electrical energy. *EPL* **2017**, *120*, 46002.
(28) Hauner, I. M.; Deblais, A.; Beattie, J. K.; Kellay, H.; Bonn, D. The Dynamic Surface Tension of Water. *J. Phys. Chem. Lett.* **2017**, *8*, 1599−1603.
(29) Biesheuvel, P. M.; Lange, F. F. Application of the Charge Regulation Model to the Colloidal Processing of Ceramics. *Langmuir* **2001**, *17*, 3557−3562.
(30) Kim, B.-S.; Harriott, P. Critical entry pressure for liquids in hydrophobic membranes. *J. Colloid Interface Sci.* **1987**, *115*, 1−8.

DOI: 10.1021/acs.langmuir.8b02875
Langmuir 2018, 34, 15174−15180